

This paper was published in Optical Materials Express and is made available as an electronic reprint with the permission of OSA. The paper can be found at the following URL on the OSA website:

<http://www.opticsinfobase.org/ome/abstract.cfm?uri=ome-2-10-1306>

Systematic or multiple reproduction or distribution to multiple locations via electronic or other means is prohibited and is subject to penalties under law.

<http://dx.doi.org/10.1364/OME.2.001306>

Extending the afterglow in $\text{CaAl}_2\text{O}_4\text{:Eu,Nd}$ persistent phosphors by electron beam annealing

Philippe F. Smet,^{1,2,*} Nursen Avci,^{1,2} Koen Van den Eeckhout,^{1,2} and Dirk Poelman^{1,2}

¹LumiLab, Department of Solid State Sciences, Ghent University, Krijgslaan 281-S1, 9000 Gent, Belgium

²Center for Nano- and Biophotonics (NB-Photonics), Ghent University, Belgium

*philippe.smet@ugent.be

Abstract: White, well-crystallized and strongly persistent luminescent $\text{CaAl}_2\text{O}_4\text{:Eu}^{2+},\text{Nd}^{3+}$ powders were obtained by electron-beam annealing. The electron-beam annealing resulted in a full reduction of Eu^{3+} to Eu^{2+} , based on the luminescence spectra. Considerable grain growth was observed and the annealed powder crystallized in the monoclinic phase of calcium aluminate. The afterglow intensity was about three times this of commercially available powder and the afterglow duration extended to 10 hours, considering the 0.32mcd/m^2 photopic threshold level.

©2012 Optical Society of America

OCIS codes: (160.5690) Rare-earth-doped materials; (300.6280) Spectroscopy, fluorescence and luminescence; (160.2900) Optical storage materials; (250.5230) Photoluminescence.

References and links

1. T. Maldiney, G. Sraiki, B. Viana, D. Gourier, C. Richard, D. Scherman, M. Bessodes, K. Van den Eeckhout, D. Poelman, and P. F. Smet, "In vivo optical imaging with rare earth doped $\text{Ca}_2\text{Si}_3\text{N}_8$ persistent luminescence nanoparticles," *Opt. Mater. Express* **2**(3), 261–268 (2012).
2. P. F. Smet, D. Poelman, and M. P. Hehlen, "Focus issue introduction: persistent phosphors," *Opt. Mater. Express* **2**(4), 452–454 (2012).
3. H. H. Li, S. Yin, and T. Sato, "Novel luminescent photocatalytic deNO(x) activity of $\text{CaAl}_2\text{O}_4\text{:}(\text{Eu}, \text{Nd})/\text{TiO}_{2-x}\text{N}_y$ composite," *Appl. Catal. B* **106**(3–4), 586–591 (2011).
4. Z. W. Pan, Y. Y. Lu, and F. Liu, "Sunlight-activated long-persistent luminescence in the near-infrared from Cr^{3+} -doped zinc gallogermanates," *Nat. Mater.* **11**(1), 58–63 (2012).
5. T. Matsuzawa, Y. Aoki, N. Takeuchi, and Y. Murayama, "New long phosphorescent phosphor with high brightness, $\text{SrAl}_2\text{O}_4\text{:Eu}^{2+},\text{Dy}^{3+}$," *J. Electrochem. Soc.* **143**(8), 2670–2673 (1996).
6. K. Van den Eeckhout, P. F. Smet, and D. Poelman, "Persistent Luminescence in Eu^{2+} -Doped Compounds: A Review," *Materials* **3**(4), 2536–2566 (2010).
7. H. F. Brito, J. Holsa, T. Laamanen, M. Lastusaari, M. Malkamaki, and L. C. V. Rodrigues, "Persistent luminescence mechanisms: human imagination at work," *Opt. Mater. Express* **2**(4), 371–381 (2012).
8. T. Aitasalo, J. Holsa, M. Kirm, T. Laamanen, M. Lastusaari, J. Niittykoski, J. Raud, and R. Valtonen, "Persistent luminescence and synchrotron radiation study of the $\text{Ca}_2\text{MgSi}_2\text{O}_7\text{:Eu}^{2+}, \text{R}^{3+}$ materials," *Radiat. Meas.* **42**(4–5), 644–647 (2007).
9. J. Holsa, T. Laamanen, M. Lastusaari, M. Malkamaki, E. Welter, and D. A. Zajac, "Valence and environment of rare earth ions in $\text{CaAl}_2\text{O}_4\text{:Eu}^{2+}, \text{R}^{3+}$ persistent luminescence materials," *Spectrochim. Acta, B At. Spectrosc.* **65**(4), 301–305 (2010).
10. T. Aitasalo, J. Holsa, H. Jungner, M. Lastusaari, and J. Niittykoski, "Thermoluminescence study of persistent luminescence materials: Eu^{2+} - and R^{3+} -doped calcium aluminates, $\text{CaAl}_2\text{O}_4\text{:Eu}^{2+}, \text{R}^{3+}$," *J. Phys. Chem. B* **110**(10), 4589–4598 (2006).
11. K. Van den Eeckhout, P. F. Smet, and D. Poelman, "Persistent luminescence in rare-earth codoped $\text{Ca}_2\text{Si}_3\text{N}_8\text{:Eu}^{2+}$," *J. Lumin.* **129**(10), 1140–1143 (2009).
12. C. K. Chang, J. Xu, L. Jiang, D. L. Mao, and W. J. Ying, "Luminescence of long-lasting $\text{CaAl}_2\text{O}_4\text{:Eu}^{2+},\text{Nd}^{3+}$ phosphor by co-precipitation method," *Mater. Chem. Phys.* **98**(2–3), 509–513 (2006).
13. J. Holsa, H. Jungner, M. Lastusaari, and J. Niittykoski, "Persistent luminescence of Eu^{2+} doped alkaline earth aluminates, $\text{MAI}_2\text{O}_4\text{:Eu}^{2+}$," *J. Alloy. Comp.* **323–324**, 326–330 (2001).
14. Y. H. Lin, Z. L. Tang, Z. T. Zhang, and C. W. Nan, "Influence of co-doping different rare earth ions on the luminescence of CaAl_2O_4 -based phosphors," *J. Eur. Ceram. Soc.* **23**(1), 175–178 (2003).
15. T. Aitasalo, J. Holsa, H. Jungner, M. Lastusaari, and J. Niittykoski, "Sol-gel processed Eu^{2+} -doped alkaline earth aluminates," *J. Alloy. Comp.* **341**(1–2), 76–78 (2002).
16. N. Avci, K. Korthout, M. A. Newton, P. F. Smet, and D. Poelman, "Valence states of europium in $\text{CaAl}_2\text{O}_4\text{:Eu}$ phosphors," *Opt. Mater. Express* **2**(3), 321–330 (2012).

17. X. Y. Chen, Z. Li, S. P. Bao, and P. T. Ji, "Porous $\text{MAl}_2\text{O}_4\text{:Eu}^{2+}$ (Eu^{3+}), Dy^{3+} ($\text{M} = \text{Sr}, \text{Ca}, \text{Ba}$) phosphors prepared by Pechini-type sol-gel method: The effect of solvents," *Opt. Mater.* **34**(1), 48–55 (2011).
18. S. W. Choi and S. H. Hong, "Size and morphology control by planetary ball milling in $\text{CaAl}_2\text{O}_4\text{:Eu}^{2+}$ phosphors prepared by Pechini method and their luminescence properties," *Mater. Sci. Eng., B* **171**(1-3), 69–72 (2010).
19. X. Q. Piao, K. Machida, T. Horikawa, and B. G. Yun, "Acetate reduction synthesis of $\text{Sr}_2\text{Si}_5\text{N}_8\text{:Eu}^{2+}$ phosphor and its luminescence properties," *J. Lumin.* **130**(1), 8–12 (2010).
20. T. Aitasalo, J. Holsa, H. Jungner, M. Lastusaari, and J. Niittykoski, "Comparison of sol-gel and solid-state prepared Eu^{2+} doped calcium aluminates," *Mater. Sci.* **20**, 15–20 (2002).
21. T. Aitasalo, J. Holsa, H. Jungner, M. Lastusaari, J. Niittykoski, M. Parkkinen, and R. Valtanen, " Eu^{2+} doped calcium aluminates prepared by alternative low temperature routes," *Opt. Mater.* **26**(2), 113–116 (2004).
22. P. Dorenbos, "Mechanism of persistent luminescence in Eu^{2+} and Dy^{3+} codoped aluminate and silicate compounds," *J. Electrochem. Soc.* **152**(7), H107–H110 (2005).
23. K. Korthout, K. Van den Eeckhout, J. Botterman, S. Nikitenko, D. Poelman, and P. F. Smet, "Luminescence and x-ray absorption measurements of persistent $\text{SrAl}_2\text{O}_4\text{:Eu,Dy}$ powders: Evidence for valence state changes," *Phys. Rev. B* **84**(8), 085140 (2011).
24. M. S. Rea, J. D. Bullough, J. P. Freyssinier-Nova, and A. Bierman, "A proposed unified system of photometry," *Lighting Res. Tech.* **36**(2), 85–111 (2004).
25. D. Poelman, N. Avci, and P. F. Smet, "Measured luminance and visual appearance of multi-color persistent phosphors," *Opt. Express* **17**(1), 358–364 (2009).
26. M. F. Zawrah and N. M. Khalil, "Synthesis and characterization of calcium aluminate nanoceramics for new applications," *Ceram. Int.* **33**(8), 1419–1425 (2007).
27. X. M. Teng, Y. H. Liu, Y. Z. Liu, Y. S. Hu, H. Q. He, and W. D. Zhuang, "Luminescence properties of Tm^{3+} co-doped $\text{Sr}_2\text{Si}_5\text{N}_8\text{:Eu}^{2+}$ red phosphor," *J. Lumin.* **130**(5), 851–854 (2010).
28. B. Lei, K. Machida, T. Horikawa, H. Hanzawa, N. Kijima, Y. Shimomura, and H. Yamamoto, "Reddish-Orange Long-Lasting Phosphorescence of $\text{Ca}_2\text{Si}_5\text{N}_8\text{:Eu}^{2+}, \text{Tm}^{3+}$ Phosphor," *J. Electrochem. Soc.* **157**(6), J196–J201 (2010).
29. F. Clabau, X. Rocquefelte, S. Jobic, P. Deniard, M. H. Whangbo, A. Garcia, and T. Le Mercier, "Mechanism of phosphorescence appropriate for the long-lasting phosphors Eu^{2+} -doped SrAl_2O_4 with codopants Dy^{3+} and B^{3+} ," *Chem. Mater.* **17**(15), 3904–3912 (2005).

1. Introduction

Persistent phosphors or afterglow materials form a specific class of luminescent compounds having the ability to emit light long after the excitation has ended. These materials find applications in emergency signage, toys, catalysis and medical imaging [1–4]. After the discovery of $\text{SrAl}_2\text{O}_4\text{:Eu,Dy}$ as efficient green persistent phosphor [5], the research has mainly focused on rare-earth doped phosphors [6,7]. Most often, Eu^{2+} is introduced as the recombination center, while the afterglow is extended by addition of other trivalent rare earth ions. In particular, Nd^{3+} , Dy^{3+} and Tm^{3+} are often the best choices, although this is still to large extent a phenomenological observation [6,8–11]. Calcium aluminate ($\text{CaAl}_2\text{O}_4\text{:Eu,Nd}$) can show a deep blue Eu^{2+} emission (peaking at 440nm) with an afterglow of several hours [12–14]. Several synthesis methods have been described besides common solid state reaction, including sol-gel, combustion, co-precipitation and microwave synthesis [12,15–18].

For europium doped persistent phosphors, care has to be taken to obtain divalent europium ions after the synthesis, which often involves thermal treatments under reducing conditions, as otherwise the trivalent state is obtained. These reducing conditions can be obtained by modification of the synthesis conditions, by using a hydrogen (or mixed nitrogen-hydrogen) atmosphere or by vacuum annealing [19–22]. Nevertheless, we have recently shown that during the charging process (i.e. the excitation of the phosphor, leading to the trapping of charges in the lattice) Eu^{3+} ions are temporarily formed [23]. In addition, phosphors showing only Eu^{2+} emission can still contain a relatively large fraction of Eu^{3+} ions [9,16].

Although the addition of specific rare earth co-dopants can be beneficial for the afterglow duration and intensity, it is difficult to actually incorporate these trivalent ions into the phosphor lattice and segregation often occurs. This is caused by the charge (and size) mismatch with the substituted alkaline earth ions. Mixing of all constituent ions at the atomic level can for instance be achieved by using sol-gel methods. We recently reported that a sol-gel based method can lead to $\text{CaAl}_2\text{O}_4\text{:Eu,Nd}$ showing persistent luminescence, if a post-annealing thermal treatment in forming gas (90% N_2 , 10% H_2) is used [16]. With this method, relatively low synthesis temperatures could be used compared to solid state synthesis.

Although this post-annealing led to an efficient reduction of the europium dopant to its divalent state, the afterglow duration and intensity was limited. This was partially ascribed to the fact that the synthesized powders turned gray after the post-annealing, probably due to the extensive formation of oxygen vacancies [16]. The gray body colour does not only lead to undesired absorption pathways, thus hampering the excitation of Eu^{2+} luminescence centers, but it also lowers the afterglow emission reaching the observer. Therefore it was necessary to explore other reducing methods. In the present work, electron beam annealing (i.e. the irradiation of the phosphor by a focused electron beam, as used for physical vapour deposition) was used as an interesting alternative treatment. Efficient and fast reduction of the Eu ions, well-crystallized powders and bright afterglow were achieved when applied to $\text{CaAl}_2\text{O}_4:\text{Eu},\text{Nd}$.

2. Experimental setup

$\text{CaAl}_2\text{O}_4:\text{Eu},\text{Nd}$ luminescent powders were prepared via a non-aqueous sol-gel method, as described in detail elsewhere [16]. In brief, $\text{CaAl}_2\text{O}_4:\text{Eu}^{3+},\text{Nd}^{3+}$ powders were synthesized using calcium nitrate tetrahydrate, hydrated europium(III) nitrate, neodymium(III) nitrate hexahydrate and aluminum sec-butoxide as precursor, n-butyl alcohol as solvent and acetylacetone as chelating agent. Very stable and transparent solutions were readily obtained via this route [16]. After heat treatment in air (1000°C , 1h), $\text{CaAl}_2\text{O}_4:\text{Eu}^{3+},\text{Nd}^{3+}$ powders with a white body colour were obtained and subsequently pressed into pellets.

In the next stage, the europium ions were reduced by electron-beam annealing, in a Leybold Univex 450 vacuum system equipped with an e-beam evaporation source (8kV, max. 400mA). At a base pressure of 2×10^{-6} mbar, the sample to be annealed was uniformly heated using a slightly defocused electron beam, until glowing white. The annealing duration was typically less than 5 s and care was taken not to melt the sample. The disc-like shape of the pellet was not deformed after the annealing.

X-ray diffraction measurements (XRD, Bruker D8-Discovery, Cu $K\alpha$ radiation, 40kV, 40mA) were used to obtain information about the crystal structure. Photoluminescence emission and excitation and afterglow duration were measured with a FS920 luminescence spectrometer (Edinburgh Instruments). Absolute afterglow measurements were performed with a photometer (International Light Technologies ILT1700) calibrated for a photopic eye response.

Scanning electron microscopy (Hitachi, S3400-N) was used to study the morphology of the phosphors. To avoid charging, measurements were performed at a pressure of 25Pa, and a back-scattered electron detector was used. The local chemical composition was studied with energy-dispersive x-ray analysis (EDX). An ultradry EDX detector (Noran 7, Thermo Scientific) with an energy resolution of 129eV was used. For the EDX analysis, an electron beam accelerating voltage of 15kV was used. Ca-K, Al-K, Nd-L and Eu-L lines were followed for the elemental analysis.

3. Results and discussion

Figure 1 shows the emission spectrum of the $\text{CaAl}_2\text{O}_4:\text{Eu},\text{Nd}$ powder after the sol-gel synthesis and heat treatment in air (for 1h) at 1000°C , i.e. after the first steps of the synthesis process. This emission spectrum almost entirely consists of line emission from the internal $4f^6$ transitions in Eu^{3+} , with only a weak blue contribution related to Eu^{2+} . XANES (x-ray absorption near-edge spectroscopy) showed earlier that approximately 55% of all europium ions are in the trivalent state in this stage of the synthesis process [16]. After e-beam annealing of this powder material, the emission spectrum is solely composed of the broad Eu^{2+} emission band typical for monoclinic $\text{CaAl}_2\text{O}_4:\text{Eu}$, peaking at 440 nm (Fig. 1). No traces of Eu^{3+} emission in the e-beam annealed powder were detected, even though the emission spectrum was recorded using 260nm excitation, which coincides with the charge transfer

transition for Eu^{3+} . Furthermore, by using 465nm, i.e. directly in the ${}^7\text{F}_0$ - ${}^5\text{D}_2$ transition of Eu^{3+} , no Eu^{3+} emission could be detected either.

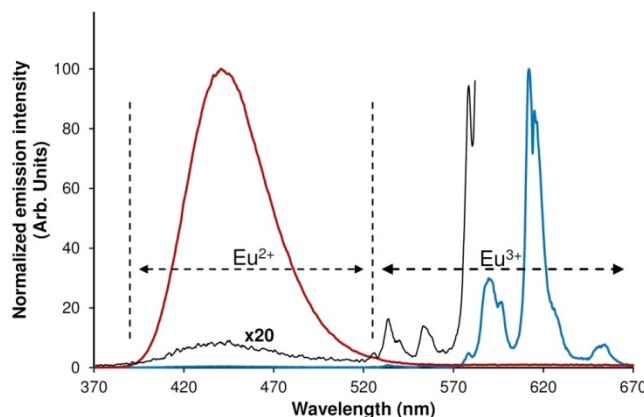


Fig. 1. Normalized PL emission spectra of $\text{CaAl}_2\text{O}_4:\text{Eu}$ (1%) heat-treated at 1000°C before (blue and black lines) and after (red line) post-annealing using electron beam. The emission spectra are recorded at room temperature at an excitation wavelength of 260nm.

Therefore, we can state that this annealing method yields pure Eu^{2+} emission. More importantly, it also provides a white body color, in contrast to post-annealing under H_2/N_2 atmosphere [16]. This is important in order to avoid absorption losses and consequently achieve efficient excitation of the Eu ions and high emission intensity.

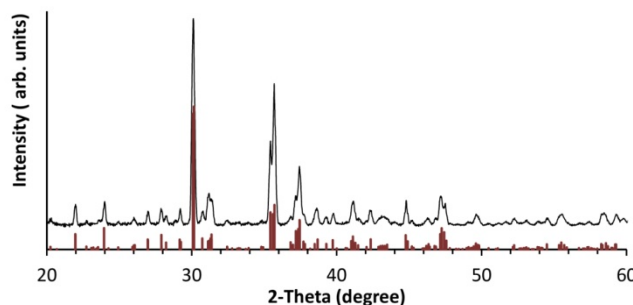


Fig. 2. X-ray diffraction pattern (black line) for e-beam annealed $\text{CaAl}_2\text{O}_4:\text{Eu},\text{Nd}$. The reference pattern for monoclinic CaAl_2O_4 (01-070-0134) is indicated in red.

The e-beam annealing not only provides a white body colour, it also leads to the formation of the monoclinic CaAl_2O_4 phase (Fig. 2), which has been shown to be beneficial for the afterglow intensity [21]. No impurity phases are detected in the x-ray diffraction pattern. The phase transition from the hexagonal phase (as present in the powders heat treated in air) to the monoclinic phase is complete. Furthermore, the narrow diffraction peaks, in combination with a much increased signal-to-noise ratio as compared to this for powder prior to the e-beam annealing, suggest a full crystallization of the powder after e-beam annealing. These crystallographic changes are also reflected in the morphology. Scanning electron microscopy images (Fig. 3) confirm the crystalline nature of the material, as large grains with well-defined crystal facets are observed. The typical dimensions are about $10\text{ }\mu\text{m}$. This is in strong contrast to the morphology before electron-beam annealing (Fig. 3), where irregularly shaped grains of various size are obtained.

After annealing, brighter areas are seen in between grains. In these areas, a strongly increased concentration of neodymium and europium was found by means of EDX (energy dispersive x-ray analysis). The large atomic number of the rare earth ions (compared to the

constituent atoms of the CaAl_2O_4 host lattice) leads to an increased probability to observe back-scattered electrons, giving rise to a stronger signal in the scanning electron image, hence forming the brighter areas. Figure 3 (bottom) shows a line scan across such a grain boundary, clearly indicating a strongly increased Nd and Eu concentration. By performing a systematic inspection of grain boundaries, it was found that the Nd concentration was typically somewhat larger than the Eu concentration. Due to the specific morphology of precipitates in between grain boundaries and the relatively large interaction volume at the used electron beam energy (15keV), it was not possible to determine the exact composition of the precipitates.

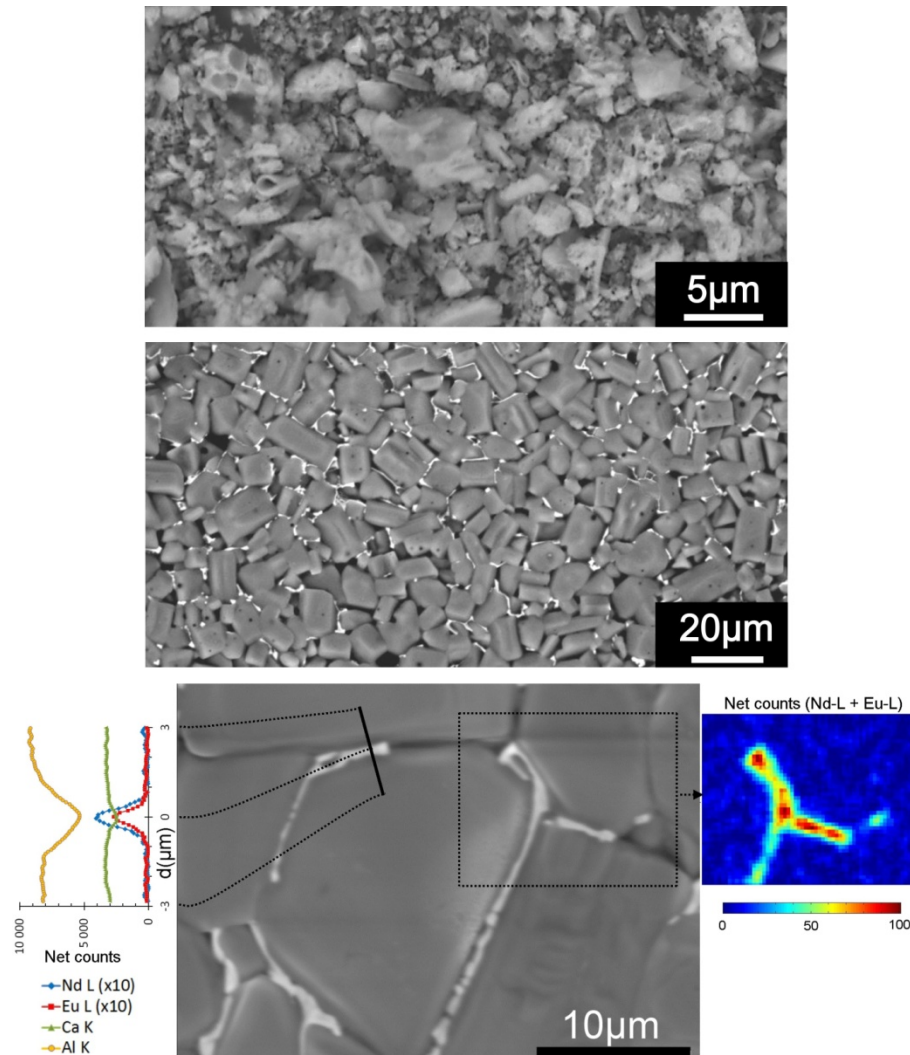


Fig. 3. Scanning electron microscopy image of $\text{CaAl}_2\text{O}_4\text{:Eu,Nd}$, before **(top)** and after **(middle)** the e-beam annealing, using back-scattered electrons. **(bottom)** Enlarged area of the e-beam annealed powder, showing a line scan across a grain boundary and a mapping of the rare earth elements using EDX.

After exposing e-beam annealed $\text{CaAl}_2\text{O}_4\text{:Eu,Nd}$ pellets to sun-light or ultraviolet light, they show a strong, violet to blue afterglow emission. The emission can be perceived by the dark-adapted eye for more than 72h. To quantify the decay behavior, a commercially available CaAl_2O_4 -based persistent phosphor (GloTech International) was pressed into a pellet of similar dimensions. Figure 4 shows the emission intensity (monitored at 450nm) of both types

of pellets upon excitation during 6 minutes with monochromatic light of 350nm in the FS920 spectrometer. Samples were kept in the dark for a sufficiently long time prior to the experiment (more than five days), so that all traps which are relevant for the afterglow process at room temperature can be assumed to be empty. Clearly, the light emission intensity during the excitation is not constant, but smoothly increases, until saturation is reached. This build-up in the luminescence is associated with the competitive process of filling the traps responsible for the afterglow. Although the steady-state luminescence intensity of the e-beam annealed pellet is somewhat lower than that of the commercially available phosphor, the afterglow of the former is about three times as high as that of the latter one. This ratio is more or less constant throughout the afterglow, except for the first tens of seconds. Note that the luminescence intensity during the excitation for the e-beam annealed pellet is not yet fully saturated after an excitation of 6 minutes.

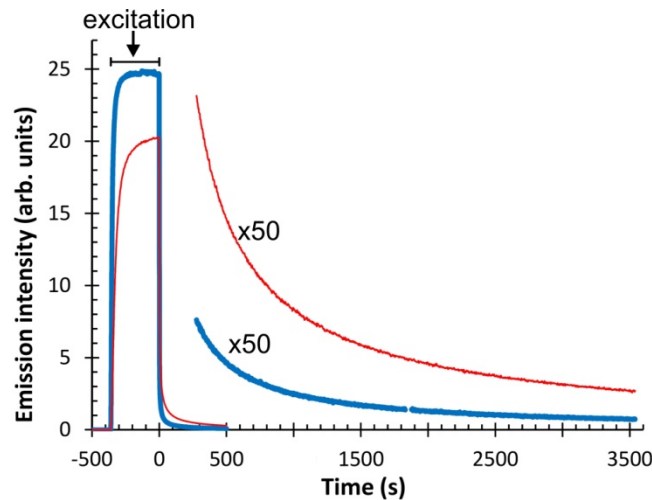


Fig. 4. Emission intensity monitored at 450nm for benchmark $\text{CaAl}_2\text{O}_4\text{:Eu,Nd}$ (blue line) and e-beam annealed $\text{CaAl}_2\text{O}_4\text{:Eu,Nd}$ (red line). The samples are excited at 350nm for 360s. The excitation ended at time $t = 0$ s.

The absolute light output of the e-beam annealed samples was measured and compared to selected benchmark persistent phosphors which are commercially available (Fig. 5). The samples, as disc-like pellets, were exposed to 1000lux of unfiltered light from a Xe arc source. The absolute afterglow intensity was measured as a function of time with a sensitive photometer (ILT 1700, using photopic mode). The afterglow duration is then defined as the time for the light output to reduce to 0.32mcd/m^2 . For the benchmark $\text{CaAl}_2\text{O}_4\text{:Eu,Nd}$ sample this is 3.1 hours, while for the sample prepared by sol-gel synthesis and e-beam annealing this amounts to 10.8 hours. The afterglow intensity of the latter is on average between 3 to 4 times higher than for the benchmark phosphor with similar composition, which is in line with the results shown in Fig. 4.

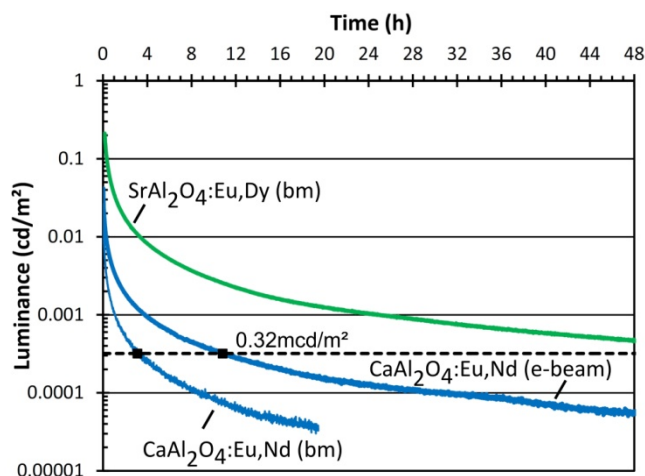


Fig. 5. Absolute luminance of $\text{CaAl}_2\text{O}_4\text{:Eu,Nd}$ and $\text{SrAl}_2\text{O}_4\text{:Eu,Dy}$ persistent phosphors measured after excitation for 10 minutes with 1000 lux of unfiltered light from a Xe arc source. (bm): benchmark phosphor, (e-beam): phosphor prepared in this work using e-beam annealing.

From Fig. 5, it is clear that the afterglow intensity of the green-emitting $\text{SrAl}_2\text{O}_4\text{:Eu,Dy}$ benchmark phosphor is still significantly higher than that of the e-beam annealed $\text{CaAl}_2\text{O}_4\text{:Eu,Nd}$ (on average a factor of 10), when using the photopic luminance (in cd/m^2) as a measure. This unit takes the human eye sensitivity explicitly into account, and is valid for use in bright light conditions [24,25]. Expressed in number of emitted photons per second, the afterglow intensity of the e-beam annealed $\text{CaAl}_2\text{O}_4\text{:Eu,Nd}$ is about 80% of this for the benchmark $\text{SrAl}_2\text{O}_4\text{:Eu,Dy}$. Therefore we can state that the calcium aluminate phosphor is a viable alternative if emission in the blue part of the spectrum is required. Also in the case where the afterglow is detected by the human eye in dark-adapted conditions, this phosphor is interesting as in these conditions its emission spectrum matches very well with the scotopic light sensitivity curve, thus yielding an increase in perceived brightness. It was verified that its emission could easily be observed with the unaided, dark-adapted eye for 72 hours after the excitation.

It is clear that e-beam annealing as a post-synthesis treatment leads not only to brighter afterglow in $\text{CaAl}_2\text{O}_4\text{:Eu,Nd}$, but also induces profound structural changes. We now discuss the three main effects, and their possible mechanism.

First of all, the powders are well-crystallized in the monoclinic phase. This is probably due to the relatively high temperatures reached during the e-beam annealing, so that one can rapidly heat to close to or slightly above the melting temperature (1400°C , [26]). This is considerably higher than in common furnace based temperature treatments (typically $1000\text{--}1200^\circ\text{C}$). The phase formation in the $\text{CaO-Al}_2\text{O}_3$ system is known to be complex, and long reaction times are required to obtain crystallization in the desired stoichiometry under conventional heating [26]. Also the fast cooling can be beneficial to quench a certain crystallographic situation.

Second, the powders are white and the reduction from Eu^{3+} (as present in the starting powder) to Eu^{2+} appears to be complete, judging from the emission spectrum. The electron-beam annealing is performed in vacuum, and can be considered as *mildly* reducing, in contrast to the *strong* reduction when annealing in a hydrogen containing atmosphere. Therefore, one can achieve by e-beam annealing the reduction of Eu – also helped by the high temperature – without the extensive formation of defects, such as oxygen vacancies, which are leading to undesired absorption.

The third important observation deals with the presence of the rare earth dopants in precipitates, as found at the grain boundaries. Both the dopant (Eu) and the co-dopant (Nd) are

detected, although the latter in higher concentration, presumably due to the charge mismatch of Nd^{3+} with Ca^{2+} . This obviously lowers the actual rare earth concentration in the bulk of the phosphor grains, although its extent could not be quantified. The optimum effective dopant concentration is not a priori clear, as often no obvious trend is observed between the afterglow intensity and the concentration of dopants and co-dopants [6,27,28]. The increased afterglow intensity could be related to a more homogeneous spatial distribution of the traps, to altered trap depths or to a decrease of non-radiative recombination channels. An interesting tool which can be used in future research is thermoluminescence (TL) spectroscopy, as more details on trap depth and distribution can be extracted. Preliminary TL experiments indicate that the glow peaks are highly dependent on excitation wavelength, excitation intensity and temperature during excitation, which means that interpretation is far from straightforward, and the full study of TL in these materials is outside of the scope of this work.

4. Conclusions

We found that electron-beam annealing is a viable option to reduce the europium ions in $\text{CaAl}_2\text{O}_4\text{:Eu,Nd}$ powders. It leads to well-crystallized powders, having a long and bright afterglow. The differences between this method and standard thermal treatments in vacuum or in reducing atmosphere are a much faster heating, a higher temperature, short dwell time and fast cooling. Clearly, the white body colour and the full crystallization are beneficial for the afterglow intensity.

It is clear that more research is required to elucidate not only the role of co-dopants in the trapping mechanisms in persistent phosphors [2,10,22,29], but also to pinpoint why electron-beam annealing is beneficial for this compound. Further improvements to the annealing method are situated in a better control of the heating profile (peak temperature, duration and cooling rate). The method was also briefly tested for a few other persistent phosphors. Preliminary results indicate that it performs well for the green-emitting $\text{SrAl}_2\text{O}_4\text{:Eu,Dy}$, but not for the orange-emitting $\text{Ca}_2\text{Si}_5\text{N}_8\text{:Eu,Tm}$.

Acknowledgments

KVdE thanks the BOF-UGent for financial support. This research is partially supported by the Interuniversity attraction poles programme IAP/VI-17 (INANOMAT) financed by the Belgian State, Federal science policy office.